First observations of ELM triggering by injected lithium granules in EAST

2013 Nucl. Fusion 53 113023

(http://iopscience.iop.org/0029-5515/53/11/113023)

Nucl. Fusion **53** (2013) 113023 (7pp) doi:10.1088/0029-5515/53/11/113023

First observations of ELM triggering by injected lithium granules in EAST

D.K. Mansfield[1], A.L. Roquemore[1], T. Carroll[1], Z. Sun[2], J.S. Hu[2], L. Zhang[2], Y.F. Liang[3], X.Z. Gong[2], J.G. Li[2], H.Y. Guo[2], G.Z. Zuo[2], P. Parks[4], W. Wu[4] and R. Maingi[4]

[1] Princeton Plasma Physics Laboratory, PO Box 451, Princeton, NJ 08543, USA
[2] Institute for Plasma Physics, Chinese Academy of Sciences, Hefei 230031, People's Republic of China
[3] Forschungszentrum Julich GmbH, Association EURATOM-FZ Julich, Institut fur Plasmaphysik, Trilateral Euregio Cluster, D-52425 Julich, Germany
[4] General Atomics, San Diego, CA 92121, USA

E-mail: dmansfield@pppl.gov

Received 28 May 2013, accepted for publication 6 September 2013
Published 27 September 2013
Online at stacks.iop.org/NF/53/113023

Abstract
The first results of edge-localized mode (ELM) pacing using small spherical lithium granules injected mechanically into H-mode discharges are reported. Triggering of ELMs was accomplished using a simple rotating impeller to inject sub-millimetre size granules at speeds of a few tens of meters per second into the outer midplane of the EAST fusion device. During the injection phase, ELMs were triggered with near 100% efficiency and the amplitude of the induced ELMs as measured by Dα was clearly reduced compared to contemporaneous naturally occurring ELMs. In addition, a wide range of granule penetration depths was observed. Moreover, a substantial fraction of the injected granules appeared to penetrate up to 50% deeper than the 3 cm nominal EAST H-mode pedestal width. The observed granule penetration was, however, less deep than suggested by ablation modelling carried out after the experiment. The observation that ELMs can be triggered using the injection of something other than frozen hydrogenic pellets allows for the contemplation of lithium or beryllium-based ELM pace-making on future fusion devices. This change in triggering paradigm would allow for the decoupling of the ELM-triggering process from the plasma-fuelling process which is currently a limitation on the performance of hydrogen-based ELM mitigation by injected pellets.

1. Introduction

Large transient events, including edge-localized modes (ELMs), are problematic for future high power fusion devices, such as ITER, because of the associated large periodic heat loads on plasma-facing components [1]. Two methods to address this issue are (1) elimination of large ELMs altogether with, for example, 3D magnetic perturbations, or (2) rapid controlled triggering of small ELMs thus creating more manageable transient heat loads. One proven method for ELM triggering involves periodic injection of high-speed cryogenic deuterium pellets [2–5]. The use of fuel pellets, however, introduces the prospect of increased plasma density; and while recent research has nearly eliminated density increases, the flexibility to use pellet materials other than fuel is still desirable [6].

The Experimental Advanced Superconducting Tokamak (EAST) is a fusion facility ($R \sim 1.8$ m, $a \sim 0.4$ m) located in Hefei, China and is designed to produce reactor-relevant long-pulse (eventually 10^3 s) discharges. Recently, EAST research has focussed on employing lithium (Li) wall coatings together with different heating techniques in order to produce and study a wide variety of H-mode discharges [7, 8].

In this work the use of small slow Li granules to trigger ELMs in EAST H-mode plasmas is reported for the first time. Spherical, sub-millimetre size Li granules were mechanically injected into the EAST midplane using a simple air motor to rotate a two-blade plastic impeller and thus impart the horizontal injection velocity. Hence, this technology facilitated the shallow and controlled penetration of Li 'pellets' into the H-mode pedestal region.

Owing to incomplete diagnostic coverage, however, no claim of power loading mitigation is made in this initial work.

2. The injector hardware

A simple apparatus was developed for the repetitive, low-speed injection of small commercially available spherical Li

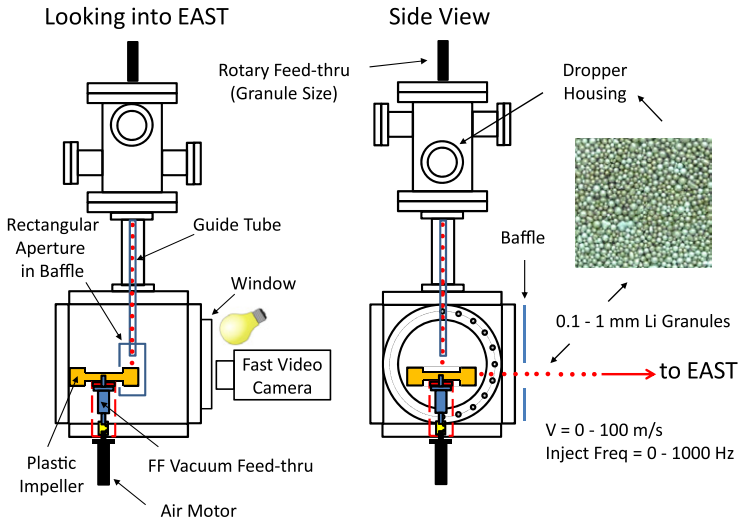

Figure 1. Two schematic views of the injector hardware used in this work. Pre-sorted spherical Li granules falling through a narrow guide tube were struck by the blades of a rotating plastic impeller. The granules were thus redirected horizontally at higher speeds through a rectangular aperture in a baffle and into the midplane of EAST H-mode target discharges. Monitoring of the granule-impeller impacts as well as the subsequent granule ablation was accomplished with a side-viewing fast video camera.

granules. The apparatus employed in this work allows for the injection of selected granule diameters in the range ∼0.1–1 mm. Further, the system is capable of controlling injection velocities in the ∼0–100 m s^{-1} range and achieving *mechanical* injection frequencies approaching 700 granules per second for 1 mm granule diameters and several thousand granules per second for smaller (0.1–0.9 mm) sizes. The injector apparatus consisted of two parts: (1) a dropper device with a guide tube and (2) a horizontally rotating plastic impeller powered by an air motor driving a high-speed (up to ∼270 Hz shaft frequency) ferrofluidic (FF) vacuum feedthrough (see figure 1).

The dropper device used in this work was similar to that used to inject a Li aerosol, in the form of ∼40 μm spherical Li powder, into the scrape-off layers of fusion devices and is described in detail elsewhere [8, 9]. Briefly, the dropper employed a 0.4 mm thick piezoelectric disc (PZD) with 64 mm diameter and a 2.5 mm central aperture. When the PZD was driven into mechanical resonance by a low-voltage audio oscillator operating at ∼2.25 kHz, spherical Li particles exiting a reservoir and residing on the surface of the disc were compelled to fall through the aperture at a rate approximately proportional to the oscillator voltage.

A thin tube with 4 mm inside diameter was precisely centred and positioned less than 1 mm below the PZD exit aperture. The tube was used to guide falling particles to a point ∼5 mm above the rotating impeller blades. The height of the guide tube (0.44 m) was chosen to ensure that the vertical speed of the falling granules (3.0 m s^{-1}) would allow them to penetrate deeply into the impact column under the guide tube and just in front of the impeller surface between appearances of sequential blades. This deep penetration, in turn, ensured reasonable *unsynchronized* mechanical efficiency of injection (95% at the design point: 1 mm spheres with an injection speed of 50 m s^{-1} requiring 150 Hz shaft frequency). Further, the narrowness of the guide tube ensured a reasonably small spread in the granule injection angle as the particles crossed the EAST separatrix which was 2.00 m distant from the impeller axis for the discharges discussed below.

As seen in figure 1, a video camera with 15 kHz framing rate was used to document granule injection events. Using the video data, it was possible to record the effects of individual Li granules on the plasma and to make measurements of individual granule velocities as well as the apparent depths of granule penetration into the plasma pedestal. This recording is demonstrated in figure 2. In this example from shot 42477 are shown a sequence of video images that capture an impeller blade striking a falling granule. Also seen is a rectangular 'flash' on the structure at the bottom of the guide tube. This light results from the ablation of the injected granule which back-illuminates the rectangular aperture in the nearby baffle (shown in figure 1). The granule time-of-flight (TOF) to the pedestal was determined by the delay between the time of impeller impact and the *start* of ablation (i.e. the timing of the first frame that exhibited back-illumination of the rectangular aperture—image (*d*) in figure 2). Because the distance between the impeller axis and the last closed flux surface was known, the granule velocity could be determined by TOF. This measured velocity was then checked for self-consistency with the velocity calculated from the video images of the spinning impeller. In all cases, self-consistency was found within the uncertainties of the respective velocity measurements (±1.8%).

The TOF (30–130 ms depending on which discharge was under study and in particular 38.06–44.26 ms for shot 42477 discussed below) of each individual injected granule was recorded—as was the start and end times of each 'flash' emitted from ablating granules as they entered the plasma edge. The duration of each ablation 'flash' (400–900 μs for shot 42477) together with the velocity determined by TOF were then used to calculate the apparent depths of granule penetration into the plasma pedestal and are discussed in section 4.3.

3. Target plasmas H-mode parameters

Figure 3 shows a typical EAST H-mode target discharge employed in this work. The target discharges were run in

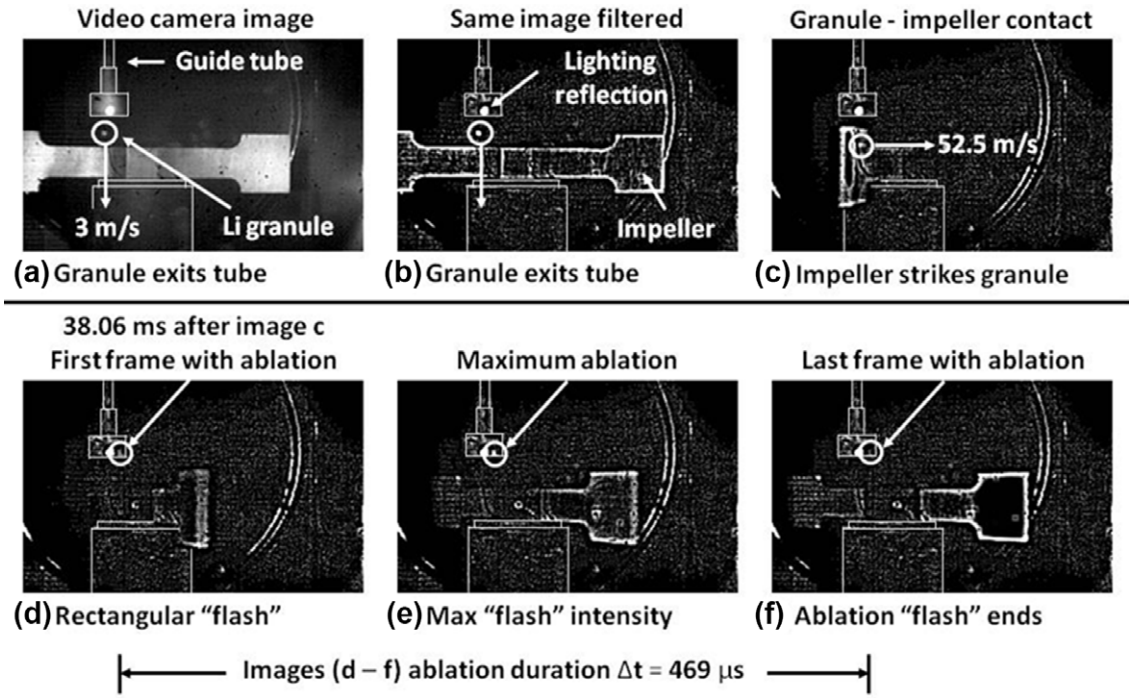

Figure 2. In this sequence of video images are shown: (*a*) an unfiltered view of the tenth granule falling from the guide tube at 3 m s^{-1} as the impeller was spinning with a velocity at the point of contact of 52.5 m s^{-1}, (*b*) the effects of applying digital filtering to (*a*), (*c*) the impeller striking the granule and imparting a horizontal velocity of ∼52.5 m s^{-1}, (*d*)–(*f*) the appearance and disappearance of a rectangular 'flash' on the structure at the bottom of the guide tube—indicating ablation of the granule. For this particular granule the measured TOF was 38.06 ms and the calculated granule penetration depth was 2.5 cm.

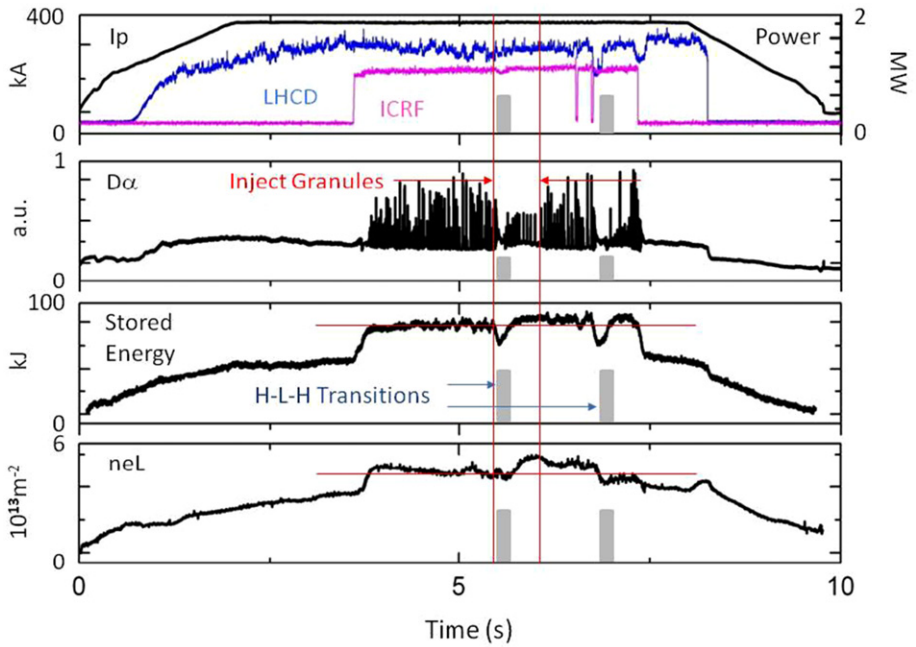

Figure 3. Global plasma parameters for EAST H-mode shot 42477. Li granules were injected for approximately one second during the period indicated by the vertical red lines. The third injected granule appeared to cause a brief (∼0.1 s) H–L–H transition followed by a period during which essentially all ELMs were triggered by Li granules. It may be seen that robust naturally occurring ELM activity was present both before and after the one-sec-long injection of Li granules. The grey areas are indications of the two H–L–H transitions discussed in the text.

lower-single-null configuration ($T_i(0) \sim T_e(0) \sim 1$ keV) with both lower hybrid current drive (LHCD) and ion cyclotron radio frequency (ICRF) heating. The particular H-mode discharge shown had parameters similar to several other contemporaneous discharges and exhibited similar behaviours in reaction to injected Li granules in the 25–70 m s^{-1} range. These discharges were in a naturally occurring mixed ELM regime with both large and small ELMs observed before and

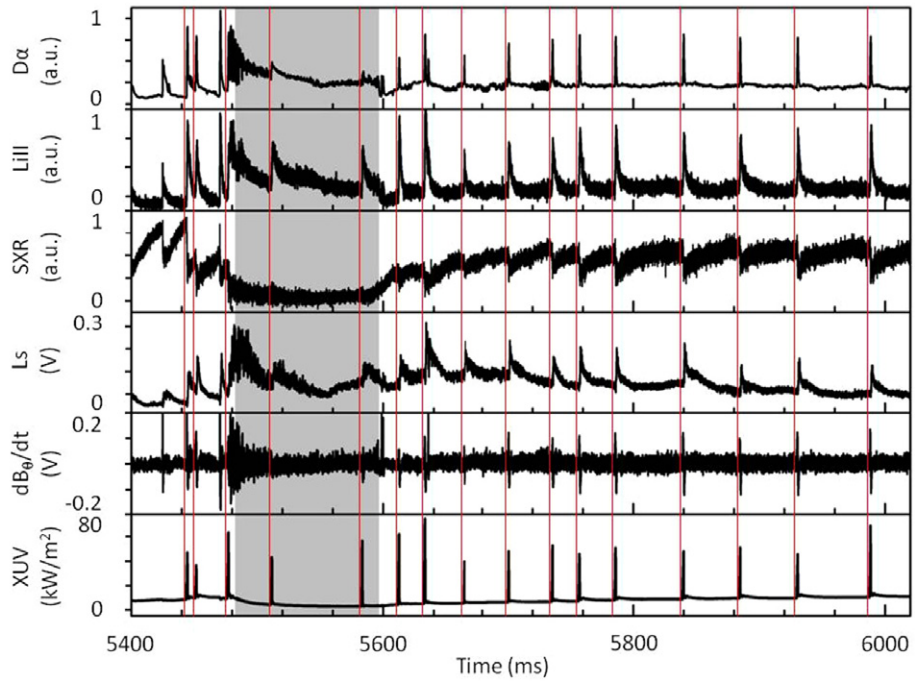

Figure 4. An expanded view of the granule injection phase during shot 42477. Included are traces of multiple diagnostics typically used to establish the presence or absence of ELM activity. They are in descending order: D-alpha emission, Li II emission, edge soft x-ray emission, divertor Langmuir probe signal, Mirnov coil signal and edge XUV emission. Red vertical lines have been drawn from the leading edge of each edge XUV emission event (bottom trace) and superimposed over all other data. The use of this signal for such timing purposes is based on the fact that sharp XUV emission was observed to correspond with the entry of a granule into the plasma edge whether or not the discharge was in the H- or L-mode. Granules 17 and 18 are not shown in this diagram. The grey area encompasses the H–L–H transition brought on by the third injected granule.

after Li granule injection. The large ELMs exhibited lower frequencies ($\sim 10^1$–10^2 Hz) while the smaller ELMs exhibited higher frequencies similar to the Type III ELMs as described previously in EAST [8]. (The mixed nature of the target plasma ELMs can be best seen by reference to the Dα traces in figure 5 below).

4. Results of Li injection experiments

4.1. ELM triggering

In the data shown in figure 3 for shot 42477, Li granules with nominal diameter 0.7 ± 0.1 mm were injected with $\sim$25 Hz repetition rate from $t = 5.4$–6.4 s. In this example the injection velocity was held fixed at $51.53 \pm 0.93\,\mathrm{m\,s^{-1}}$ (see section 4.3 below) and the injected granules were observed to trigger ELMs with essentially 100% efficiency as indicated by the Dα spikes shown between vertical red lines. As can be seen, the ELMs triggered by Li injection caused smaller Dα perturbations than those caused by contemporaneous ELMs occurring naturally in shot 42477.

Following a dithering H–L transition period brought on by the injection of the third granule (of eighteen in 42477) and represented by the grey area(s) in figure 4, an H-mode was re-established in which all subsequent injected granules successfully triggered ELMs. Also, in this example modest increases in stored energy and line average electron density were observed during the course of granule injection.

Using the fast video camera, individual apparent granule penetration depths past the separatrix were measured to vary from 2–4.5 cm (section 4.3). Drawing on edge Thompson scattering and reflectometry measurements, the pedestal pressure width for shot 42477 was estimated to be 3 cm with $\Delta T_e \sim 0.34$ keV [10, 11]. Because the third granule initiated an otherwise-ELM-free H–L–H transition, it seems reasonable to conclude that the penetration for that particular granule was larger than optimal—presumably because the chosen granule size was too large. Indeed, the measured apparent penetration of the third granule in this example was 4 cm—slightly beyond the top of the pedestal.

It should also be noted that there are two clear H–L–H transitions represented in figure 3. The first transition appears to be coincident with the arrival of the third Li granule and the triggering of a large ELM. The second transition occurred well after the cessation of granule injection and the subsequent return to naturally occurring ELM activity. This second transition is mentioned only to point out that the target H-mode plasma was vulnerable to spontaneous return to L-mode. It is also possible that the latter transition could have been caused by a brief drop in input power.

4.2. Injection timing versus ELM timing and machine diagnostic observations

As can be seen in figure 4, the first two granules were injected into a robustly ELMing H-mode. Coincident with the entry of the third granule (following a large naturally occurring ELM) the discharge left the H-mode and briefly ($\sim$100 ms) entered a dithering L-mode before re-establishing the H-mode with an ELM-free period. During this brief H–L excursion, two

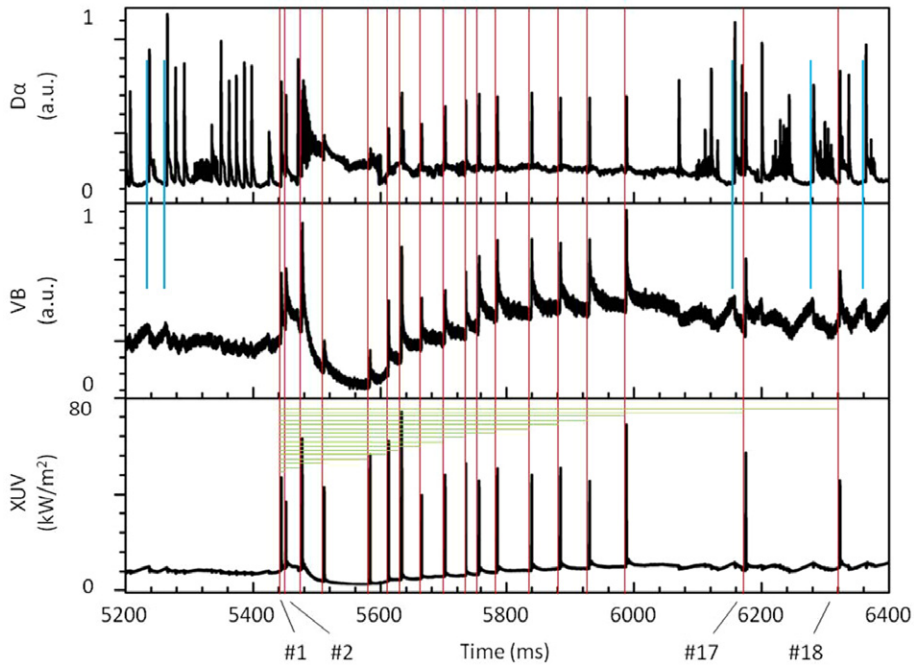

Figure 5. Shown from top to bottom are signals of divertor Dα, edge tangential VB and XUV emissions. As in figure 4, red vertical lines originating from the leading edge of the XUV signals are used to landmark triggered ELMs. Blue vertical lines indicate some naturally occurring ELMs. The green horizontal lines were generated independently from the video associated with this discharge and indicate the time of injection from the first granule.

more granules entered the plasma column and did not result in ELM-like signatures (note, for example, the absence of an MHD signal). Subsequently, after the plasma resumed the H-mode all of the observed ELMs except one were coincident with the injection of Li granules.

There are other interesting aspects of the ELM data. For example, shown in figure 5 are traces of divertor Dα, tangential edge visible bremsstrahlung (VB), and tangential edge extreme ultra-violet (XUV) from shot 42477. Shown superimposed over this data—in order to guide the eye—are red and blue vertical lines indicating the leading edges of all triggered and a few naturally occurring ELMs, respectively. Also superimposed over the XUV data are horizontal green lines. The length of each of these lines was determined independently from the video images discussed above and indicates the timing of each of the injected Li granules with respect to the first injected granule. As can be seen, the video system was able to account extremely well for every granule injected.

Additional features can be seen in figure 5. In particular, at least for 0.7 mm granules, the edge XUV signal appeared to be a reliable and crisp timing indicator of granule entry into the plasma boundary whether L-mode or H-mode obtained. This property may prove useful in future experiments at higher injection frequencies during which timing and accounting by video may not be practical. Another feature to note is that there is a clear difference in the behaviour of the tangential VB signals in response to naturally occurring ELMs and Li-triggered ELMs. As seen in the figure there were four granules injected during a period of naturally occurring ELMs (two just before the H–L–H transition—granule 1 and 2—and two well afterwards—granules 17 and 18). In each case (and in all cases of injection into the ELM-free period—granules 6–16) the resulting VB signal exhibited a sharp leading edge and slowly decreasing trailing edge. In contrast, for all cases of naturally occurring ELMs, the opposite occurred i.e. a slowly increasing leading edge was followed by a sharply decreasing trailing edge. This property may also prove useful in future experiments involving granule injection into ELMing discharges.

4.3. Granule/impeller speeds and the apparent depth of pedestal penetration

Shown in figure 6 is a histogram of the measured TOF for all granules injected into 42477. As shown, all injected granules, except #6, had essentially the same TOF (mean TOF $= 38.81 \pm 0.71$ ms—excluding granule #6). Hence, all granules in shot 42477 except #6 entered the plasma edge with the same nominal radial velocity of $51.53 \pm 0.93\ \mathrm{m\,s^{-1}}$.[5]

[5] On the video, rather than being struck cleanly, granule #6 was seen to rebound off the top of an impeller blade as that blade passed under the guide tube. The rebounding granule then fell in front of the *next* impeller blade but not directly under the guide tube. Rather, the point of granule impact was displaced several millimetres radially inwards from the tube (i.e. towards EAST). This displacement ensured that granule #6 did not enter the plasma directly, but rather, could only have entered by ricocheting off the left edge of the baffle as represented in figure 1. Granule #6 did, in fact, enter the plasma and trigger an ELM. Because it did not do so with a well-defined radial velocity, however, it was excluded from the considerations and discussion about triggering ELMs at constant radial velocity.

This type of off-normal contact of a granule with an impeller blade (a miss-hit) can be remedied in several ways. Among the possible solutions to this problem are: (1) reducing the dimensions of the baffle aperture (figure 1) so as to reduce the effective angle-of-acceptance for renegade granules and (2) the most effective solution—simple synchronization of the falling granules with the rotating impeller so as to ensure that no rebounds or miss-hits occur. Synchronization is certainly possible in future generations of the hardware described above; but it was not considered necessary for the proof-of-principle experiment outlined in this work.

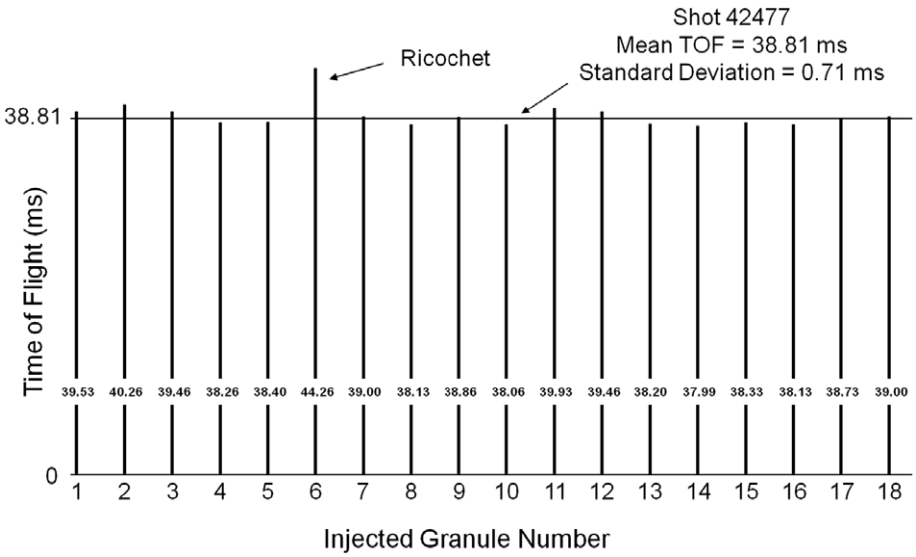

Figure 6. A histogram of the measured TOF data for shot 42477. Granule #6 was not struck cleanly by the impeller and thus entered the plasma after ricocheting off of the left edge of the baffle shown in figure 1. All other granules entered the pedestal region with essentially the same radial velocity.

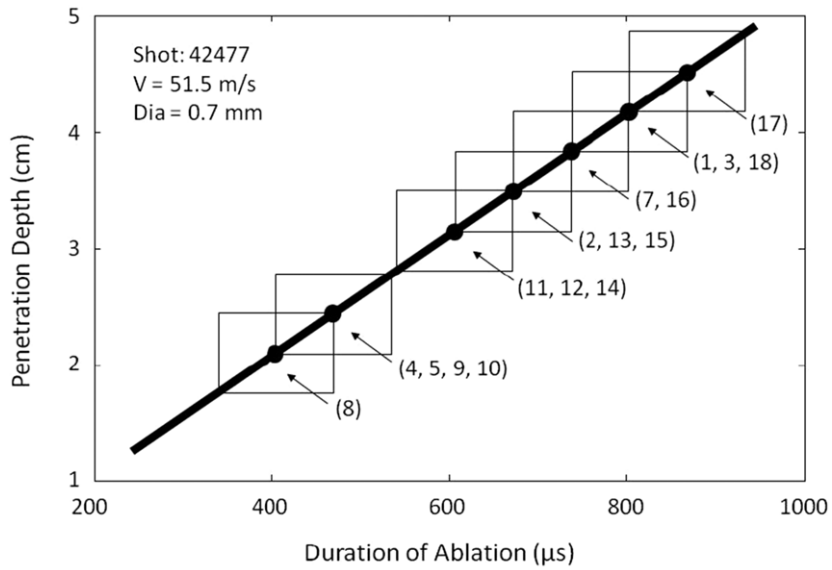

Figure 7. The apparent penetration depths of all granules injected into shot 42477. The width of each data box represents the uncertainty in the measurement of ablation time (i.e. twice the 67 μs sampling time of the video images). The height represents the uncertainty of the penetration measurement assuming 51.5 m s^{-1} granule velocity. The associated granule number is also shown for each of the injected granules—excluding #6. The nominal pedestal width for shot 42477 was 3 cm.

This observation enabled a crude measurement of the apparent penetration depth of each injected granule to be undertaken.

As shown in figure 7, in order to measure depth of penetration, a straight line with slope 51.53 m s^{-1} was drawn on a graph of distance versus time. This represents the measured constant radial velocity of the injected granules. The measured durations of ablation (with uncertainty $\pm 67\,\mu$s—the video camera framing time) were then fitted over the line of constant velocity and a depth of penetration was assigned to the ordinate.

Several features of the data can be noted: (1) the observed penetration depths are roughly equal to the width of the pressure pedestal ($\sim$3 cm) as determined by independent estimate; (2) there is a significant spread in the apparent penetration depths (2–4.5 cm); (3) granule #3, which initiated a brief H–L–H transition is among the most deeply penetrating granules and, in fact, appears to have penetrated beyond the pedestal width—as did others.

5. Discussion and conclusions

ELMs have been triggered successfully and in a controlled manner using low velocity Li granules during H-mode discharges on the EAST tokamak. It is interesting to note that the triggered ELMs observed in this work had smaller Dα amplitudes (albeit lower frequency) than the naturally occurring ELMs exhibited by the target plasmas. This

observation bodes well for the technique that was tested in this work.

The main difference in design between the dropper used in this work and that described in [9] is that, in this work, the chamber used to store Li spheres was segmented into four independent reservoirs. The design allows a 'door' to be rotated into place which accesses any one of the four reservoirs and thus introduces different size granules (pre-sorted and stored in different reservoirs) onto the PZD surface. Granule size selection could thus be accomplished externally by manually rotating a vacuum feedthrough as shown in figure 1. In this work the Li granules loaded into the dropper reservoir segments were pre-sorted into 0.9, 0.7, 0.5 and 0.3 mm diameters (±0.1 mm) using calibrated metallic meshes. This choice of granule sizes was made by drawing on calculations done *previous* to the experiment. The expected penetration of mm-scale Li granules at velocities of several tens of metres per second into a steep hypothetical H-mode pedestal was used as a beginning point for choosing a range of granule sizes. The following pedestal parameters were used in the initial calculations: width $\Delta r \sim 4$ cm, $\Delta T_i \sim \Delta T_e \sim 1.0$ keV, $\Delta n_e \sim 5.0 \times 10^{13}$ cm^{-3}.

Using the initial calculations as a guide, granules with 0.7 mm nominal diameter were chosen for the initial attempt at ELM triggering because it was *conjectured* that these granules would penetrate deeply into the EAST H-mode pedestal at velocities in the neighbourhood of 50 m s^{-1}. It was hoped that the scaling of penetration depth with granule size could be investigated by changing granule sizes during the initial experiments. Due to limited run time, however, only the dropper segment housing 0.7 mm granules was accessed during the initial proof-of-principle experiments presented in this work.

During the experiment, the apparent penetration depths measured as described above were generally deeper than the estimated pedestal width (~3 cm). In addition, calculations done *after* the experiment and based on the EAST shot 42477 nominal pedestal parameters ($\Delta r \sim 3$ cm, $\Delta T_i \sim \Delta T_e \sim 0.34$ keV, $n_e \sim 2.5 \times 10^{13}$ cm^{-3}) indicated that the depth of penetration should have been even larger than observed [12, 13]. These inconsistencies could be caused, in part, by the unconventional method by which the apparent penetration depths were measured. It is possible, for example, that the assumption of constant granule speed in the pedestal is unjustified. More experiments with different granule sizes and a sophisticated suite of edge diagnostics are needed to resolve these inconsistencies.

It is particularly important that the minimum penetration depth needed to trigger an ELM be determined in future work. It is also important to understand whether, as has been discussed, the occasional H–L–H transitions caused by granule injection can be eliminated by the use of smaller or slower granules. It is hoped that the full ranges of granule size, speed and pacing frequency permitted by the injector can be accessed in future EAST run campaigns.

Li coatings have been used successfully to eliminate ELM activity on NSTX [14–17]. The lack of ELM 'flushing' activity, however, has led to the rapid accumulation of impurities in the core. Although there is no measurement available of the central Li concentration for the discharges studied in this work, there is ample evidence in the literature demonstrating that externally introduced Li does not accumulate in the core of fusion devices [18–22]. Future plans include installation of similar injection hardware on NSTX-U which will have the ability to measure core Li concentrations directly via charge-exchange recombination spectroscopy [22, 23]. The use of Li granules to trigger small ELMs could, therefore, potentially flush the NSTX core of impurities while simultaneously replenishing Li to plasma-facing components and thus suppressing large ELMs.

Finally, the simple demonstration that ELMs can be triggered by the injection of something other than purely hydrogenic 'pellets' allows for the contemplation of ELM pacing without the addition of unwanted fuelling. Aside from Li as a granule material, it is possible to consider LiD, beryllium (Be) and perhaps compounds such as BeD_2 or $LiBeD_3$.

Acknowledgments

This work was sponsored in part by the US Department of Energy under contracts DE-AC02-09CH11466 and by the National Natural Science Foundation of China under contracts 11075185, 11021565, 11075181, 10725523, 10721505, 10990212 and the National Magnetic confinement Fusion Science Program under Contracts No 2013GB114004, 2010GB104001 and 2010GB104002. The work was also supported by the Chinese Academy of Sciences Visiting Professorship for Senior International Scientists Grant No 2012T1J0025.

The authors wish to thank Dr Larry Baylor of Oak Ridge National Laboratory, as well as Drs Marina Yakovleva and Scott Meiere of FMC Lithium Corporation for their many useful discussions and suggestions.

References

[1] Loarte A. *et al* 2003 *Plasma Phys. Control. Fusion* **45** 1549
[2] Lang P.T. *et al* 2011 *Nucl. Fusion* **51** 033010
[3] Kocsis G. *et al* 2007 *Nucl. Fusion* **47** 1166
[4] Baylor L.R. *et al* 2007 *Nucl. Fusion* **47** 1598
[5] Pacher G.W. *et al* 2011 *Nucl. Fusion* **51** 083004
[6] Baylor L.R. *et al* 2013 *Phys. Rev. Lett.* **110** 245001
[7] Wan B. *et al* 2009 *Nucl. Fusion* **49** 104011
[8] Xu G.S. *et al* 2011 *Nucl. Fusion* **51** 072001
[9] Mansfield D.K. *et al* 2010 *Fusion Eng. Des.* **85** 890
[10] Zang Q. *et al* 2011 *Rev. Sci. Instr.* **82** 063502
[11] Wang Y.M. *et al* 2013 *Fusion Eng. Des.* at press
[12] Parks P.B. *et al* 1994 *Nucl. Fusion* **34** 417
[13] Parks P.B. *et al* 1988 *Nucl. Fusion* **28** 477
[14] Mansfield D.K. *et al* 2009 *J. Nucl. Mater.* **390–391** 764
[15] Maingi R. *et al* 2009 *Phys. Rev. Lett.* **103** 075001
[16] Maingi R. *et al* 2011 *Phys. Rev. Lett.* **107** 145004
[17] Mangi R. *et al* 2012 *Nucl. Fusion* **52** 083001
[18] Mansfield D.K. *et al* 2001 *Nucl. Fusion* **41** 1823
[19] Evtikhin V.A. *et al* 2002 *Plasma Phys. Control. Fusion* **44** 955
[20] Mirnov S.V. *et al* 2006 *Plasma Phys. Control. Fusion* **48** 821
[21] Szepesi G. *et al* 2013 *Nucl. Fusion* **53** 033007
[22] Podesta M. *et al* 2012 *Nucl. Fusion* **52** 033008
[23] Bell M.G. *et al* 2009 *Plasma Phys. Control. Fusion* **51** 124054